Central European Journal of Energetic Materials, **2016**, *13*(2), 505-525
ISSN 1733-7178
e-ISSN 2353-1843

Kinetic Study of the Thermal Decomposition of Potassium Chlorate Using the Non-isothermal TG/DSC Technique

Mohsen RAVANBOD[*], Hamid Reza POURETEDAL[**], Mohammad K. AMINI, Reza EBADPOUR

Faculty of Applied Chemistry,
Malek-ashtar University of Technology, Shahin-Shahr, Iran
E-mail: [**]hr_pouretedal@mut-es.ac.ir, [*]mravanbod@mut-es.ac.ir

Abstract: The non-isothermal TG/DSC technique has been used to study the kinetic triplet of the thermal decomposition of potassium chlorate at different heating rates (5, 10, 15 and 20 °C·min^{-1}). The DSC results showed two consecutive broad exothermic peaks after melting. The first peak contains a shoulder indicating the presence of at least two processes. The overlapped peaks were resolved by a peak fitting procedure, and the three resolved peaks were used for evaluation of the kinetic triplet for each step. The TG results also showed two consecutive mass losses after melting. The kinetics of the mass loss processes were studied using resolved DTG peaks. The activation energies were calculated using the KAS model-free method. The pre-exponential factor and the best kinetic model for each step were determined by means of the compensation effect, and the selected models were confirmed by the nonlinear model fitting method. The average activation energies obtained from the DSC results were 237.3, 293.8, and 231.3 kJ·mol^{-1} for the three consecutive steps of thermal decomposition of $KClO_3$. The activation energies were 231.0 and 239.9 kJ·mol^{-1} for the first and second mass loss steps. The Avrami-Erofeev of $A_{x/y}$ with the function of $g(\alpha) = [-\ln(1-\alpha)]^{x/y}$ (x/y = 5/4 and 3/2) was the most probable model for describing the reaction steps.

Keywords: potassium chlorate, thermal decomposition, kinetic triplet, non-isothermal TG/DSC

1 Introduction

Oxidizers are usually oxygen rich ionic solids that are used in pyrotechnic and propellant compositions to facilitate the process of ignition by producing oxygen [1]. Potassium chlorate ($KClO_3$) with 39.2 wt.% oxygen content is one of the most reactive and certainly the most controversial of the common oxidizers in many pyrotechnic and propellant compositions [2]. Due to its excellent properties such as low melting point, low energy content and combustion behaviour, $KClO_3$ has been widely used in various energetic material compositions [3-7]. Also, one of the main applications of $KClO_3$ is in the production of white and coloured smokes [8, 9]. Compared with $KClO_4$, for which there are many reports on its decomposition, $KClO_3$ has not been so widely studied, nor has its decomposition behaviour been fully explained, probably because of difficulty in following its decomposition by different thermal analytical techniques [10, 11].

It has been reported that potassium perchlorate and potassium chloride are formed during the decomposition of $KClO_3$ at temperatures above its melting point. Potassium perchlorate is, in turn, decomposed to yield potassium chloride and oxygen [12, 13]. In the process of the thermal decomposition of $KClO_3$, absorption of heat increases the diffusion speed and vibration amplitude of the crystals, causing cleavage and reformation of the Cl–O bonds in $KClO_3$ with subsequent formation of stable $KClO_4$. Following this transformation, $KClO_4$ is decomposed by releasing all of its oxygen to form potassium chloride [14]. The formation of ClO^- and ClO_2^- anions, and their corresponding radicals, has also been suggested for the thermal decomposition of $KClO_3$ under gamma irradiation [15].

To the best of the authors' knowledge, no study has yet been reported on the kinetic triplets for the individual steps of the three-step decomposition process of $KClO_3$. In this regard, this study is complementary to the previous studies on the thermal decomposition of $KClO_3$. The decomposition behaviour of $KClO_3$ was studied by means of differential scanning calorimetry (DSC) and thermogravimetry (TG) under a nitrogen atmosphere. We determined the kinetic triplets, including the activation energy, the Arrhenius constant and the decomposition reaction model for each step of the three-step process of $KClO_3$ decomposition, after resolving the overlapped DSC and DTG thermograms.

The ICTAC kinetic committee recommendations [16] were used for reliable estimation of the kinetic parameters. The activation energies were calculated by the Kissinger-Akahira-Sunose (KAS) method based on DSC and TG data at different heating rates after resolution of the overlapped peaks. The compensation

effect method was then used for accurate determination of the reaction model and pre-exponential factor.

2 Experimental

Analytical grade potassium chlorate (purity > 99.9%) was purchased from Merck Company. The $KClO_3$ sample was ground in an agate mortar to produce a fine powder and then dried at 70 °C for 2 h. The particle size distribution of the $KClO_3$ powder, with a median (D_{50}) of 29.7 μm, is shown in Figure 1.

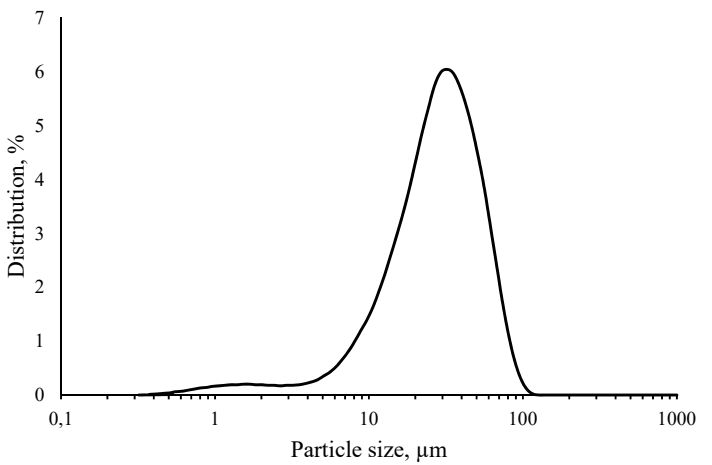

Figure 1. Particle size distribution of potassium chlorate (D_{50} = 29.7 μm).

The TG-DSC measurements were carried out using a Perkin Elmer simultaneous thermal analyzer model STA 6000 (USA). Alumina sample vessels were used (70 μL volume) with alumina powder as the reference material. A nitrogen atmosphere was applied during the analysis (flow rate of 50 mL·min^{-1}). For the kinetic study of the reactions, thermal analysis experiments were performed at different heating rates of 5, 10, 15 and 20 °C·min^{-1}. In each experiment, approximately 15 mg of $KClO_3$ was taken and heated from ambient temperature (25 °C) to 900 °C.

The particle size distribution measurements were performed using a laser particle size analyzer (FRITSCH, model Analystte 22, Micro Tec Plus).

The overlapped peaks in the DSC and DTG (differential thermogravimetry) thermograms were resolved using Peakfit v4.12 software.

3 Results and Discussion

3.1 DSC thermograms of $KClO_3$

Figure 2 shows the DSC thermograms of $KClO_3$ obtained at different heating rates (5, 10, 15, and 20 °C·min^{-1}) under a nitrogen atmosphere. The DSC thermograms show two sharp endothermic peaks and two broad successive exothermic peaks. The first endothermic peak observed around 356 °C can be assigned to melting of potassium chlorate and the second endothermic peak around 770 °C is related to melting of potassium chloride [2, 7]. The two broad consecutive exothermic peaks observed above 500 °C are due to the decomposition of $KClO_3$ [10]. The first exothermic peak which appeared as a shoulder at all of the heating rates of 5, 10, 15, and 20 °C·min^{-1} and had maximum peak temperatures of 549.7, 563.6, 571.3, and 575.5 °C, respectively, is related to the following combined reactions [17]:

$$2KClO_3 \rightarrow 2KCl + 3O_2 \quad \text{(I)}$$

$$4KClO_3 \rightarrow 3KClO_4 + KCl \quad \text{(II)}$$

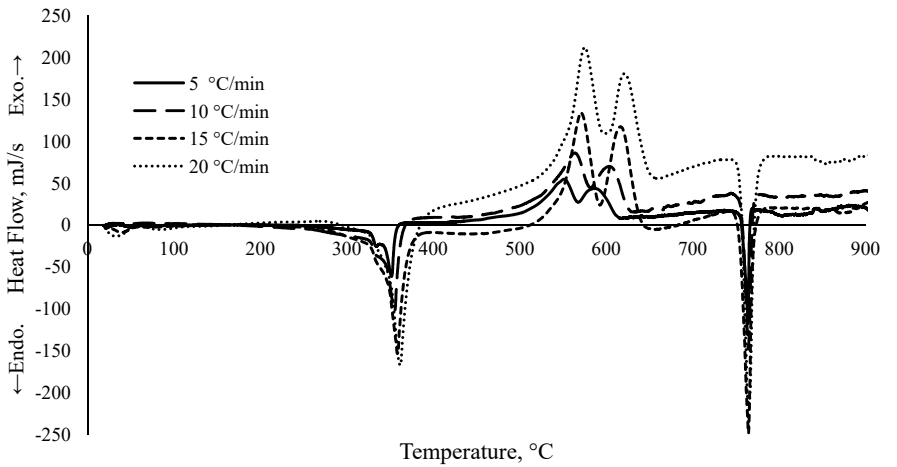

Figure 2. The DSC thermograms of $KClO_3$ at different heating rates under N_2 atmosphere.

The second exothermic peak in the DSC thermograms in Figure 2 belongs to the decomposition of $KClO_4$ according to reaction (III), which was observed at maximum peak temperatures of 586.7, 602.9, 616.3, and 621.6 °C, at heating rates of 5, 10, 15, and 20 °C·min^{-1}, respectively.

$$KClO_4 \rightarrow KCl + 2O_2 \quad \text{(III)}$$

As seen, all of the peaks shift to higher temperature with increasing heating rate, and is the basis for the kinetic calculations in thermal analysis methods.

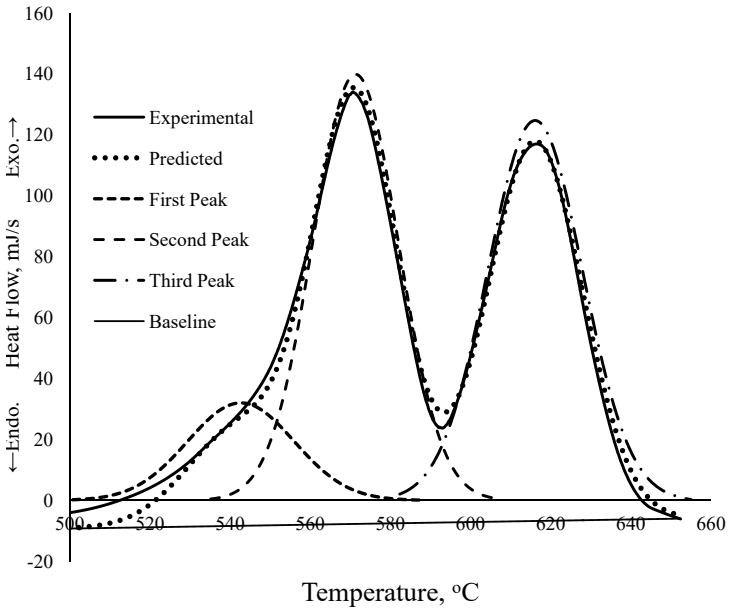

Figure 3. The three resolved peaks after curve fitting of the DSC data at a heating rate of 15 °C·min^{-1}.

Table 1. The characteristics of the DSC thermograms for three consecutive steps of $KClO_3$ decomposition at different heating rates (5-20 °C·min^{-1})

β [°C·min^{-1}]	*r^2	First step			Second step			Third step		
		T_{onset1} [°C]	T_{p1} [°C]	T_{end1} [°C]	T_{onset2} [°C]	T_{p2} [°C]	T_{end2} [°C]	T_{onset3} [°C]	T_{p3} [°C]	T_{end3} [°C]
5	0.964	467	518.4	570	510	549.7	589	554	586.7	628
10	0.966	482	533.6	587	524	563.6	603	569	602.9	643
15	0.994	494	542.7	591	535	571.3	607	584	616.3	658
20	0.996	503	548.1	593	540	575.5	611	591	621.6	662

*r^2: nonlinear regression coefficient between experiment and predicted data.

In order to evaluate the kinetic triplet for the consecutive decomposition reactions, the overlapped peaks of the DSC thermograms at different heating

rates (5, 10, 15, and 20 °C·min^{-1}) were resolved by the peak fitting procedure. The thermogram was best fitted into three resolved peaks, which provided evidence for a three-step decomposition mechanism. A typical curve fitted DSC at a heating rate of 15 °C·min^{-1} is shown in Figure 3, and the overall results at different heating rates are presented in Table 1.

3.2 TG thermograms of $KClO_3$

The TG and DTG thermograms of $KClO_3$ at three heating rates of 10, 15, and 20 °C·min^{-1} under a nitrogen atmosphere are shown in Figure 4. As for the DSC results, the TG thermograms also shift to higher temperatures with increasing heating rate. The decomposition of potassium chlorate shows two consecutive mass losses with a total mass reduction of about 40%, which is in agreement with the proposed mechanisms mentioned previously [17]. The first minor mass loss is related to reaction (I) and the major (second) mass loss is due to reaction (III). The DTG peaks were clearly resolved by the curve fitting procedure. A typical curve fitted DTG at a heating rate of 15 °C·min^{-1} is presented in Figure 5. The results for the two step mass loss and the contribution of each step at different heating rates (10, 15 and 20 °C·min^{-1}) are presented in Table 2. As seen, the contribution of the first mass loss, reaction (I), increases with increasing heating rate (16.8, 19.4, and 22.4% mass loss, for heating rates of 10, 15, and 20 °C·min^{-1}, respectively). By contrast, the contribution of the second mass loss, reaction (III) or (II), decreases at higher heating rates. Consequently, the direct decomposition of $KClO_3$ to KCl and O_2 gas, reaction (I), is enhanced with increasing heating rate.

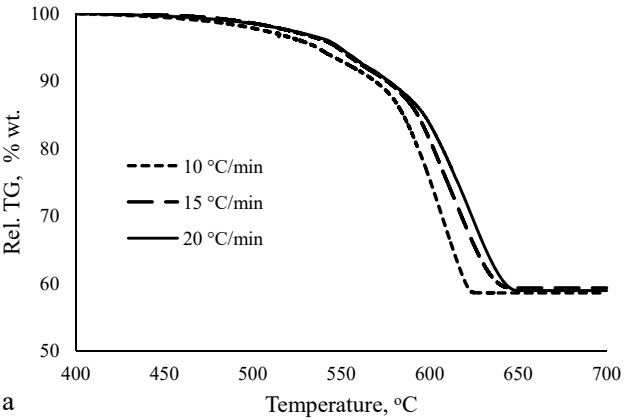

a

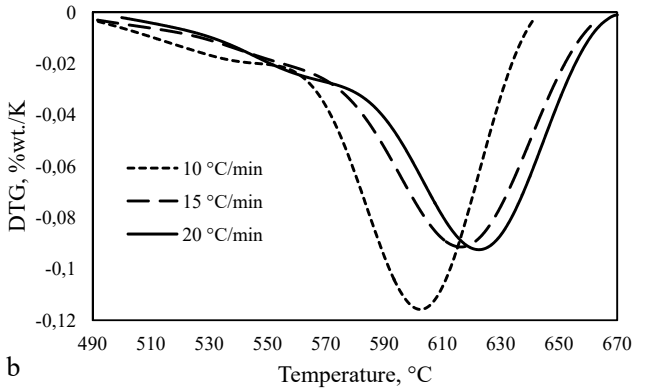

b

Figure 4. The experimental TG (a) and DTG (b) thermograms for the decomposition of $KClO_3$ at different heating rates (10, 15, and 20 °C·min^{-1}) under N_2 atmosphere.

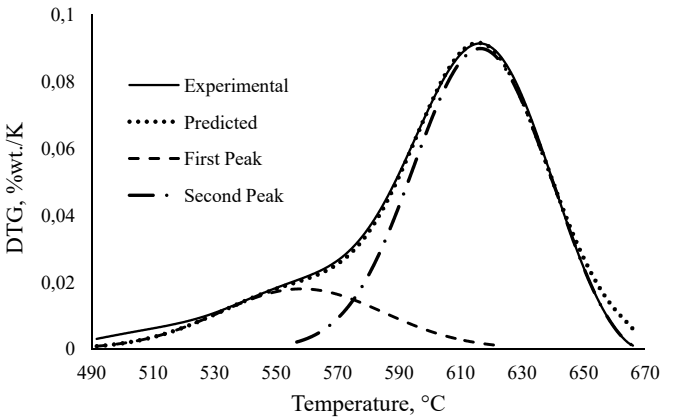

Figure 5. The two resolved peaks after curve fitting of the DTG data at a heating rate of 15 °C·min^{-1}.

Table 2. The characteristics of the DTG thermograms for the two step mass loss during $KClO_3$ decomposition at different heating rates (10, 15, and 20 °C·min^{-1})

β [°C·min^{-1}]	*r^2	First mass loss			Second mass loss			Relative peak area [%]	
		T_{onset1} [°C]	T_{p1} [°C]	T_{end1} [°C]	T_{onset2} [°C]	T_{p2} [°C]	T_{end2} [°C]	First peak	Second peak
10	0.995	485	540.6	595	549	600.8	641	16.8	83.2
15	0.996	493	550.3	608	559	610.6	658	19.4	80.6
20	0.997	501	556.4	612	564	618.3	661	22.4	77.6

*r^2: nonlinear regression coefficient between experiment and predicted data.

3.3 Kinetics of solid-state reactions

The rate of kinetic processes in the solid-state is generally a function of temperature and conversion, which can be described by the following equation:

$$\frac{d\alpha}{dt} = k(T) \cdot f(\alpha) \tag{1}$$

where α is the conversion fraction, t is time, T is absolute temperature (K) and $f(\alpha)$ is the reaction model function depending on the particular decomposition mechanism. The temperature function $k(T)$ is the "rate constant" which represents the temperature dependence of the reaction rate. The parameter $k(T)$ is usually represented by the Arrhenius relationship:

$$k(T) = A \cdot \exp[\frac{-E_a}{RT}] \tag{2}$$

where E_a is the activation energy as a function of α (kJ·mol^{-1}), R is the universal gas constant (8.314 J·mol^{-1}·K^{-1}), A (min^{-1}) is the pre-exponential (frequency) factor which is assumed to be independent of temperature and gives an idea of the association tendency of the reacting molecules [18, 19].

The activation energy E_a, the pre-exponential factor in the Arrhenius equation A, and the function of the reaction progress $f(\alpha)$ which is dependent on the decomposition mechanism, are called the kinetic triplet. The kinetic triplet is required for prediction of the thermal stability of the materials under various applied temperature conditions [20] and is needed to provide a mathematical description of the process [21].

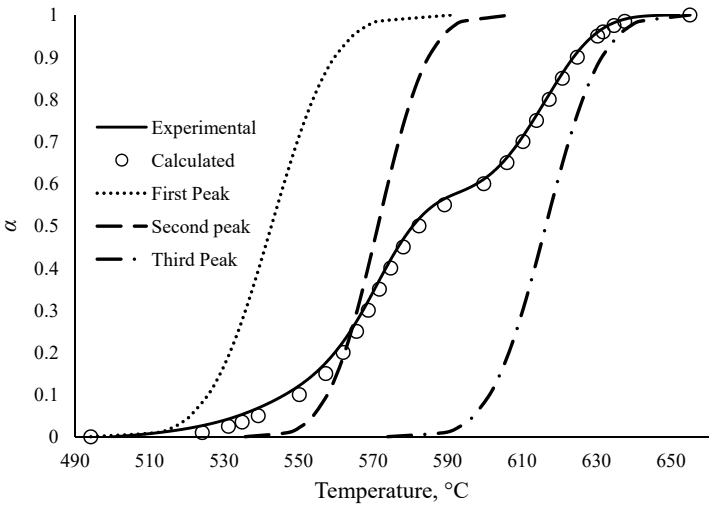

Figure 6. Individual contributions of the three decomposition steps of $KClO_3$ to the total conversion at a heating rate of 15 °C·min^{-1}.

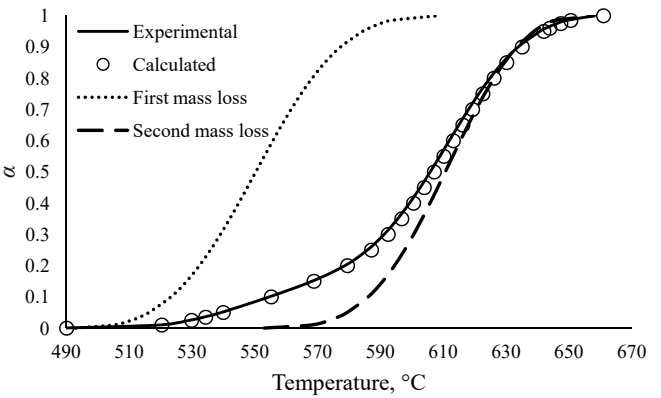

Figure 7. Individual contributions of the two step mass losses of $KClO_3$ to the total conversion at a heating rate of 15 °C·min^{-1}.

In multi-step mechanisms when the reaction profile demonstrates well separated steps under constant heating rate conditions, it is a good idea to separate the steps entirely (*e.g.*, by using peak separation methods) and to analyze their kinetics individually [16]. Figure 6 shows the individual contributions of the three

decomposition steps of $KClO_3$ to the total conversion for the DSC thermogram at a heating rate of 15 °C·min^{-1}. In addition, the individual contributions of the two mass loss steps of $KClO_3$ decomposition to the total conversion at a heating rate of 15 °C·min^{-1} is presented in Figure 7. Obviously, in all reaction profiles, the conversion fractions increase with temperature, and in adjacent α-T thermograms, the value of α_2 begins to be significant when the value of α_1 is already high. For example, as shown in Figure 7, for $\alpha_1 > 90\%$, α_2 is $< 10\%$ (about 3%) at 577 °C. In this case, as a good approximation, the decomposition of potassium chlorate in a nitrogen atmosphere can be modelled considering the reaction of each step as an independent process [22].

3.3.1 Calculation of the activation energy by a model-free isoconversional method

The KAS method [23, 24] was used to determine the activation energy of the $KClO_3$ decomposition reactions based on the conversion fractions of the DSC and DTG peak areas. This method can be expressed by the following equation:

$$\ln\left(\frac{\beta}{T^2}\right) = \text{Const} - \left(\frac{E_a}{RT}\right) \tag{3}$$

According to the above equation, plots of $\ln(\beta/T^2)$ versus $1/T$ corresponding to different extents of the conversion, α, can be obtained by linear regression using least squares methods. The activation energy E_a can be evaluated from the slope of the straight line which gives the best regression coefficients (R^2). The results of the analysis by the KAS method from four DSC measurements and three DTG measurements are presented in Figures 8 and 9, respectively. The activation energies were calculated at different heating rates via these methods for different α values in the range 0.1-0.9. The variations in the activation energies versus the conversion fraction for each of the three decomposition steps in the DSC and the two mass decreases in the DTG by the KAS method are shown in Figures 10 and 11, respectively. The average and standard deviation of the activation energies calculated by the KAS method are given in Table 3.

Table 3. The averaged activation energies (E_a, kJ·mol^{-1}) and their standard deviations for the decomposition of $KClO_3$ obtained by the KAS method

DSC [kJ·mol^{-1}]			DTG [kJ·mol^{-1}]	
First step	Second step	Third step	First mass loss	Second mass loss
237.3 ± 26.3	293.8 ± 18.7	231.3 ± 10.5	231.0 ± 7.6	239.9 ± 5.3

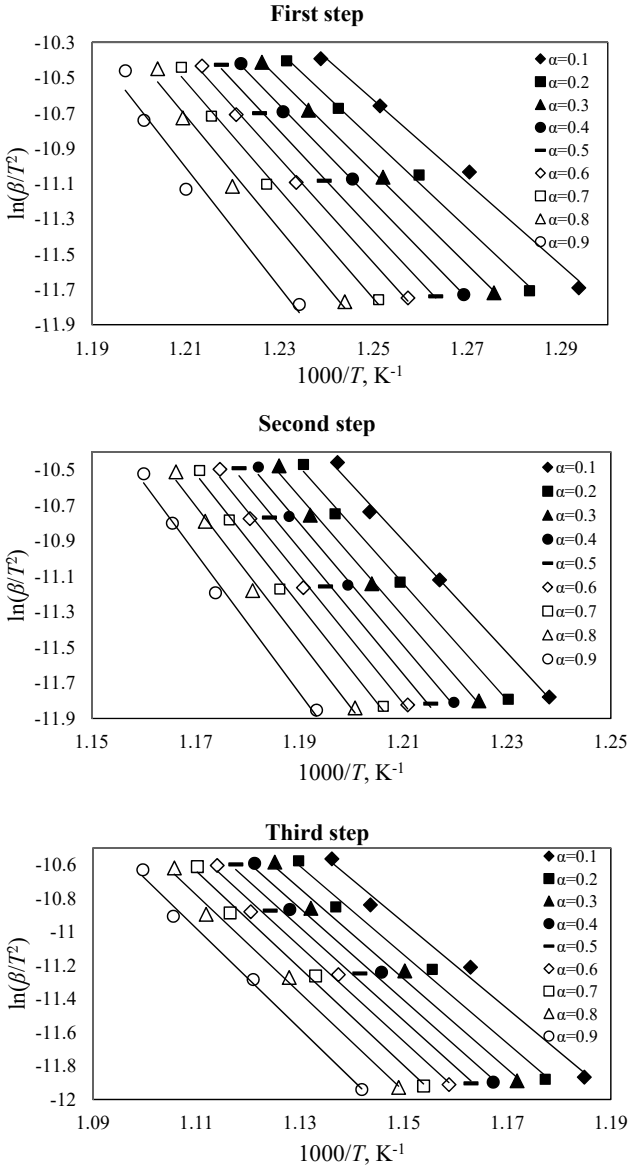

Figure 8. KAS plots for the thermal decomposition of $KClO_3$ at four heating rates and various conversions (α = 0.1-0.9, at 0.1 increments) from the DSC data.

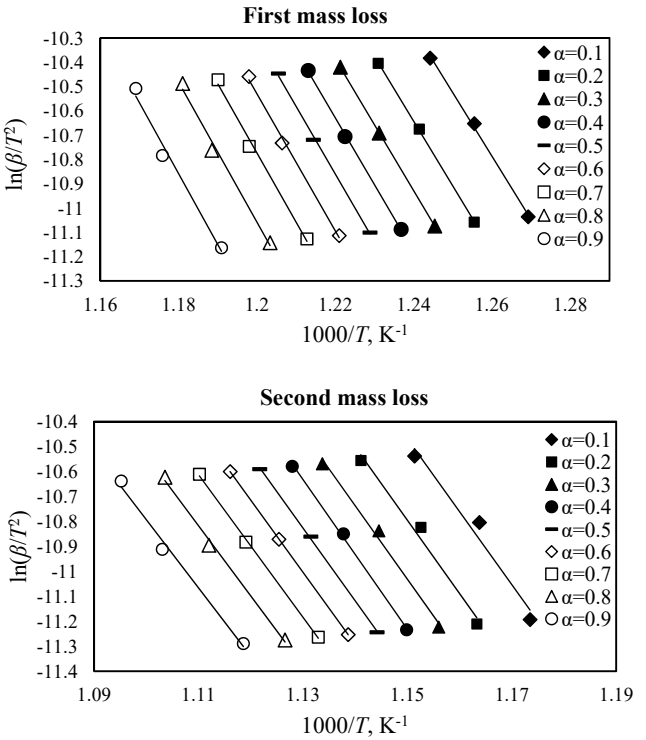

Figure 9. KAS plots for the thermal decomposition of $KClO_3$ at three heating rates and various conversions (α = 0.1-0.9, at 0.1 increments) from the DTG data.

It is clear from Table 3 that there is reasonable agreement between the activation energies of the first step in the DSC and the first mass loss in the DTG, related to reaction (I). Also the activation energies for the third DSC step and the second mass loss, related to reaction (III), are close to each other and in fact, they are not significantly different statistically. The activation energies for the decomposition of $KClO_4$ in the present work are in agreement with those reported by Lee *et al*. (231-269 kJ·mol^{-1}) [25]. The results strongly verify that the thermal decomposition of $KClO_3$ occurs according to the suggested three-step mechanism.

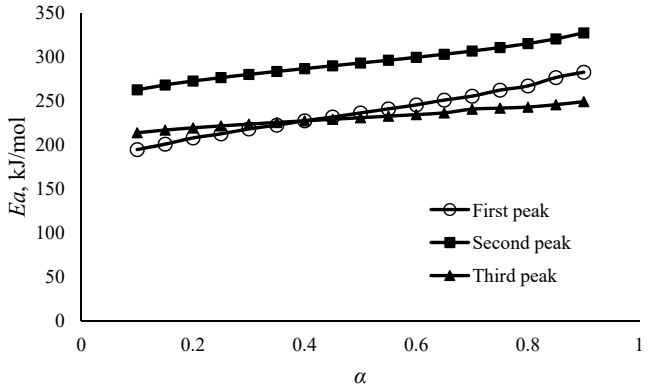

Figure 10. Dependence of the activation energies on the conversion fraction of the three decomposition steps of $KClO_3$.

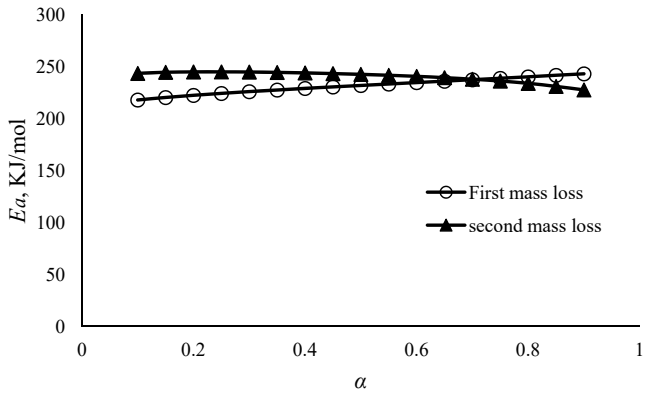

Figure 11. Dependence of the activation energies on the conversion fraction of the two mass losses in the decomposition of $KClO_3$.

3.3.2. Determination of the kinetic triplet by a model-fitting method

The kinetic parameters strongly depend on the selection of a proper mechanism function for the process. Therefore, the determination of the most probable mechanism function is highly essential [26]. It was demonstrated that the thermal decomposition of potassium chlorate occurs by a three step mechanism and two mass loss steps; these steps are completely independent. In multi-step reactions, because of the obvious differences in the reaction profiles associated with the major types of the common reaction models (*e.g*. accelerating, decelerating, and sigmoidal), determining the appropriate model type is relatively simple [16].

In order to select the reaction model for the individual steps, thirty different kinetic functions [27] of the common models in solid-state reactions (listed in Table 4) were tested with the two model fitting methods including the differential Equation 4 and the integral Equation 5 as follows [28]:

Differential method:

$$\ln\left[\frac{d\alpha/dT}{f(\alpha)[\frac{E_a(T-T_O)}{RT^2+1}]}\right] = -\frac{E_a}{RT} + \ln[\frac{A}{\beta}] \quad (4)$$

Integral equation:

$$\left[\frac{g(\alpha)}{T-T_o}\right] = -\frac{E_a}{RT} + \ln[\frac{A}{\beta}] \quad (5)$$

Table 4. Thirty types of mechanism functions $g(\alpha)$ and $f(\alpha)$ used to describe solid state reactions

No.	Differential function: $f(\alpha)$	Integral function: $g(\alpha)$
1	$1/2\ \alpha^1$	α^2
2	$-[\ln(1-\alpha)]^{-1}$	$\alpha + (1-\alpha)\ln(1-\alpha)$
3	$3/2[(1-\alpha)^{-1/3}-1]^{-1}$	$(1-2\alpha/3)-(1-\alpha)^{2/3}$
4 and 5	$3/n\ (1-\alpha)^{2/3}\ [1-(1-\alpha)^{1/3}]^{-(n-1)}$ (n=2, 1/2)	$[1-(1-\alpha)^{1/3}]^n$ (n=2, 1/2)
6	$4(1-\alpha)^{1/2}[1-(1-\alpha)^{1/2}]^{1/2}$	$[1-(1-\alpha)^{1/2}]^{1/2}$
7	$3/2(1+\alpha)^{2/3}[(1+\alpha)^{1/3}-1]^{-1}$	$[(1+\alpha)^{1/3}-1]^2$
8	$3/2(1-\alpha)^{4/3}[(1-\alpha)^{-1/3}-1]^{-1}$	$[(1/(1+\alpha))^{1/3}-1]^2$
9	$1-\alpha$	$-\ln(1-\alpha)$
10-16	$1/n(1-\alpha)[-\ln(1-\alpha)]^{-(n-1)}$ (n=1/4, 1/3, 1/2, 2/3, 4/5, 2, 3)	$[-\ln(1-\alpha)]^n$ (n=1/4, 1/3, 1/2, 2/3, 4/5, 2, 3)
17-22	$1/n(1-\alpha)-(n-1)$ (n=1/2, 1/3, 1/4, 2, 3, 4)	$1-(1-\alpha)^n$ (n=1/2, 1/3, 1/4, 2, 3, 4)
23-27	$1/n\ \alpha-(n-1)$ (n=1, 3/2, 1/2, 1/3, 1/4)	α^n (n=1, 3/2, 1/2, 1/3, 1/4)
28	$(1-\alpha)^2$	$(1-\alpha)^{-1}$
29	$(1-\alpha)^2$	$(1-\alpha)^{-1}-1$
30	$2(1-\alpha)^{3/2}$	$(1-\alpha)^{-1/2}$

According to these equations, the plots of $\ln[(d\alpha/dT)/f(\alpha)(E_a(T-T_0)/RT^2+1)]$ and $\ln[g(\alpha)/(T-T_0)]$ versus $1/T$ at different heating rates (β_s) can be obtained by linear regression. The most probable mechanism function $g(\alpha)$ is the function that affords the most linear plot with a linear regression coefficient R^2 closest to −1.000.

For accurate determination of the reaction model and pre-exponential factor, the compensation effect was used [16], and the calculated E_i and A_i values from

each of the models at different heating rates were substituted into Equation 6 to determine the compensation effect parameters a and b.

$$\ln A_i = aE_i + b \tag{6}$$

The pre-exponential factor A_o was calculated by substitution of the calculated E_o from the model free method and the a and b parameters in Equation 7:

$$\ln A_o = aE_o + b \tag{7}$$

The calculated results are presented in Table 5. The E_o and A_o values were substituted into Equation 8.

$$f(\alpha) = \beta\left(\frac{d\alpha}{dT}\right)_\alpha \left[A_o e^{\left(\frac{-E_O}{RT_\alpha}\right)}\right]^{-1} \tag{8}$$

Table 5. The kinetic triplet of the $KClO_3$ decomposition steps obtained by using model-fitting and compensation methods

Step No.	β [°C·min^{-1}]	Mechanism function, $g(\alpha)$	E_i [kJ·mol^{-1}]	ln A_i [min^{-1}]	R^2	E_O [kJ·mol^{-1}]	ln A_O [min^{-1}]	RSS
First mass loss	10	$[-\ln(1-\alpha)]^{4/5}$	191.4	26.32	0.993	231.0	32.89	0.48
	15		185.7	25.37	0.995			0.39
	20		198.6	27.52	0.993			0.55
Second mass loss	10	$[-\ln(1-\alpha)]^{3/2}$	211.9	27.40	0.994	239.9	31.68	0.98
	15		188.0	23.90	0.995			0.74
	20		206.0	26.71	0.994			0.95
First step	5	$[-\ln(1-\alpha)]^{4/5}$	293.1	43.06	0.993	237.3	34.50	0.05
	10		314.1	44.79	0.992			0.04
	15		361.3	51.87	0.993			0.22
	20		432.4	62.41	0.992			1.10
Second step	5	$[-\ln(1-\alpha)]^{3/2}$	297.1	42.25	0.993	293.8	41.65	0.065
	10		311.6	43.61	0.993			0.082
	15		354.2	49.31	0.993			0.025
	20		360.8	50.08	0.993			0.096
Third step	5	$[-\ln(1-\alpha)]^{3/2}$	233.8	31.69	0.998	231.3	31.24	0.57
	10		246.6	32.81	0.998			0.39
	15		271.6	35.74	0.998			0.45
	20		277.8	36.40	0.999			0.19

The calculated numerical values of $f(\alpha)$ were compared with the theoretical

dependencies obtained from the $f(\alpha)$ equations (*e.g.*, Table 4) to identify the best matching model. By applying this method to all of the reaction models, the mechanism function of Avrami-Erofeev $A_{5/4}$ was found to be the best pattern for reaction (I) and the mechanism function of Avrami-Erofeev $A_{3/2}$ appeared as the best one for reactions (II) and (III); these functions afforded minimum differences between the experimental and the theoretical data. The plots of the theoretical and experimental $f(\alpha)$ versus α at different heating rates for each of the three reactions are presented in Figure 12.

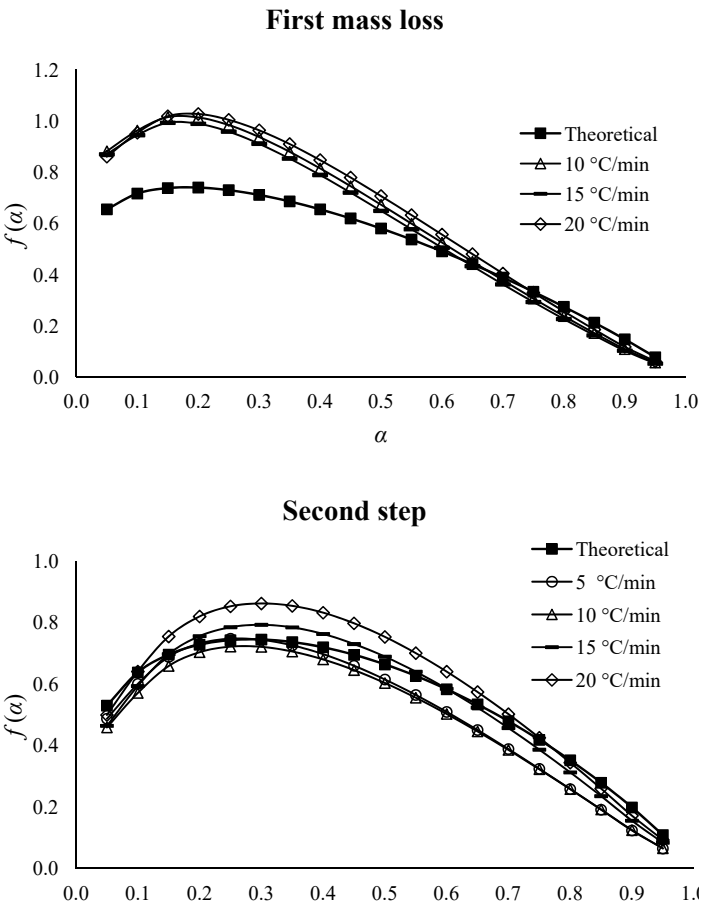

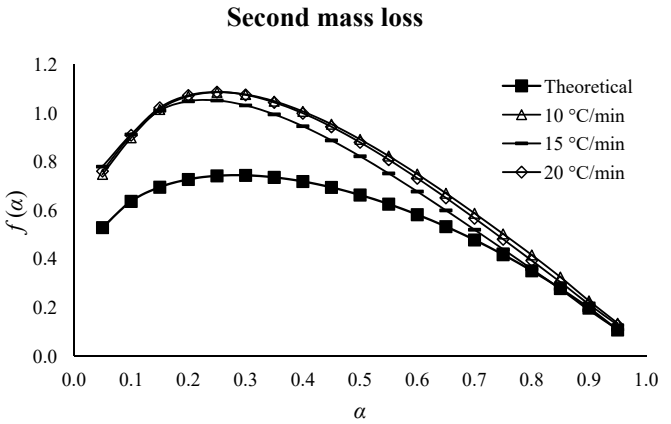
Second mass loss
Theoretical
10 °C/min
15 °C/min
20 °C/min
f(α)
α
0.0
0.2
0.4
0.6
0.8
1.0
1.2
0.0 0.1 0.2 0.3 0.4 0.5 0.6 0.7 0.8 0.9 1.0

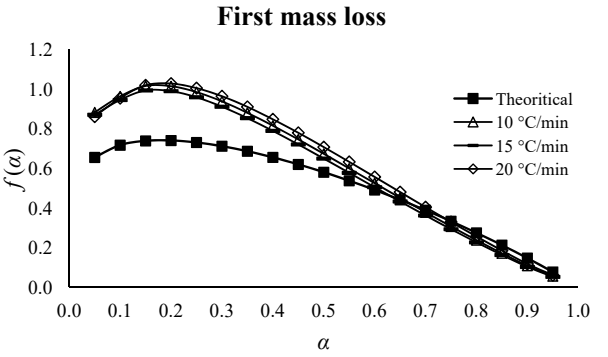
First mass loss
Theoritical
10 °C/min
15 °C/min
20 °C/min
f(α)
α
0.0
0.2
0.4
0.6
0.8
1.0
1.2
0.0 0.1 0.2 0.3 0.4 0.5 0.6 0.7 0.8 0.9 1.0

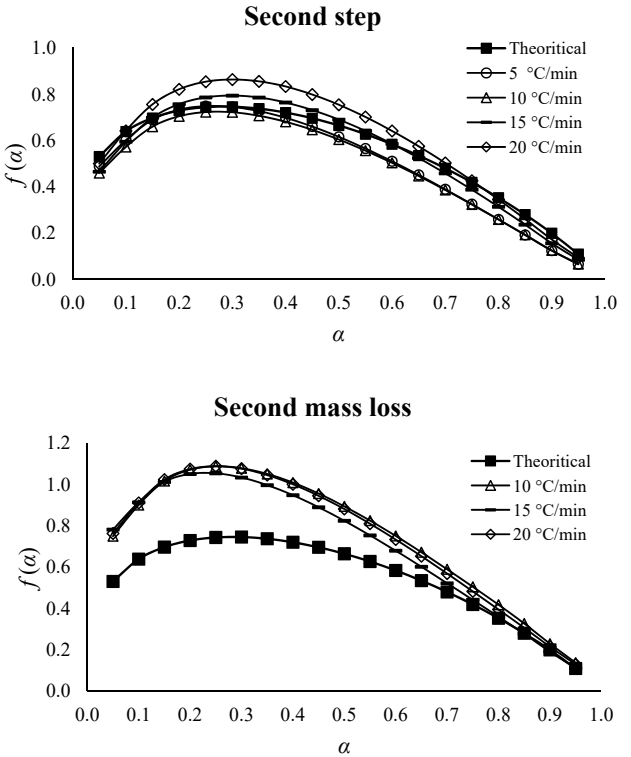

Figure 12. Plots of the theoretical and experimental $f(\alpha)$ against various conversions (α = 0.05-0.95, at 0.05 increments) at different heating rates.

The difference between the theoretical and experimental $f(\alpha)$ was calculated by means of a non-linear regression method using residual sum of squares (RSS) that should be a minimum according to Equation 9:

$$\text{RSS} = \sum(f(\alpha)_{\text{exp.}} - f(\alpha)_{\text{theor.}})^2 \rightarrow \quad \text{minimum} \tag{9}$$

The RSS values that show the minimum difference between the experimental and theoretical $f(\alpha)$, presented in Table 5, verify the chosen reaction model. Based on the results, it can be concluded that the mechanism function with the integral forms $g(\alpha) = [-\ln(1-\alpha)]^{4/5}$, $g(\alpha) = [-\ln(1-\alpha)]^{2/3}$, and $g(\alpha) = [-\ln(1-\alpha)]^{2/3}$ related to reactions (I), (II), and (III), respectively, describe the thermal decomposition of $KClO_3$. In these types of mechanisms, it was assumed that nucleation and subsequent decomposition occurred on the surface of the crystals.

4 Conclusions

The thermal behaviour of potassium chlorate was studied by means of the non-isothermal TG/DSC technique at different heating rates. The DSC thermograms exhibit two consecutive broad exothermic peaks and the DTG results exhibit a two-step mass decrease after melting. After resolving the overlapped peaks, the reaction profiles demonstrated well separated steps under constant heating rate conditions, indicating that the reaction steps are independent processes, so their kinetic triplets were analyzed individually. The results strongly imply that a three-step mechanism with a two-step mass loss is operative for the thermal decomposition of $KClO_3$.

The activation energy for each step was computed by the isoconversional KAS method. The average activation energies from the DSC results were 237.3, 293.8, and 231.3 kJ·mol^{-1} for reactions (I), (II), and (III), respectively. The values for the first and the second mass losses were 231.0 and 239.9 kJ·mol^{-1}, respectively. The Avrami-Erofeev of $A_{5/4}$ with functions of $g(\alpha) = [-\ln(1-\alpha)]^{4/5}$ and $f(\alpha) = 5/4(1-\alpha)[-\ln(1-\alpha)]^{1/5}$ can be used to show the first reaction step (first mass loss). But the Avrami-Erofeev of $A_{3/2}$ with functions $g(\alpha) = [-\ln(1-\alpha)]^{2/3}$ and $f(\alpha) = 3/2(1-\alpha)[-\ln(1-\alpha)]^{1/3}$ is the most probable mechanism for a description of the third reaction step (second mass loss) and the second reaction step of the decomposition of $KClO_3$. There is good agreement between the DSC and DTG kinetic parameters. Investigation of the DTG peak area shows that the contribution of the first step increases with increasing heating rate (16.8, 19.4, and 22.4% mass loss for heating rates of 10, 15, and 20 °C·min^{-1}, respectively).

Acknowledgement
We would like to thank the research committee of Malek-ashtar University of Technology (MUT) for supporting this work.

References

[1] Pouretedal H.R., Ravanbod M., Kinetic Study of Ignition of Mg/$NaNO_3$ Pyrotechnic Using Non-isothermal TG/DSC Technique, *J. Therm. Anal. Calorim.*, **2015**, *119*, 2281-2288.
[2] Conking J.A., Chemistry of Pyrotechnics Basic Principles and Theory, New York, Marcel Dekker INC, **1985**, p. 55; ISBN 978-1574447408.
[3] Shamsipur M., Pourmortazavi S.M., Fathollahi M., Kinetic Parameters of Binary Iron/Oxidant Pyrolants, *J. Energ. Mater.*, **2012**, *30*, 97-106.

[4] Pourmortazavi S.M., Hajimirsadeghi S.S., Hosseini S.G., Characterization of the Aluminum/Potassium Chlorate Mixtures by Simultaneous TG-DTA, *J. Therm. Anal. Calorim.*, **2006**, *84*, 557-561.
[5] Dong X.-F., Yan Q.-L., Zhang X.-H., Cao D.-L., Xuan C.-L., Effect of Potassium Chlorate on Thermal Decomposition of Cyclotrimethylenetrinitramine (RDX), *J. Anal. Appl. Pyrolysis*, **2012**, *93*, 160-164.
[6] Liao L.-Q., Yan Q.-L., Zheng Y., Song Z.-W., Li J.-Q., Liu P., Thermal Decomposition Mechanism of Particulate Core-shell $KClO_3$-HMX Composite Energetic Material, *Indian J. Eng. Mater. Sci.*, **2011**, *18*, 393-398.
[7] Hosseini S.G., Pourmortazavi S.M., Hajimirsadeghi S.S., Thermal Decomposition of Pyrotechnic Mixtures Containing Sucrose with either Potassium Chlorate or Potassium Perchlorate, *Combust. Flame*, **2005**, *141*, 322-326.
[8] Moretti J.D., Sabatini J.J., Shaw A.P., Chen G., Gilbert R.A., Jr., Oyler K.D., Prototype Scale Development of an Environmentally Benign Yellow Smoke Hand-held Signal Formulation Based on Solvent Yellow 33, *ACS Sustainable Chem. Eng.*, **2013**, *1*, 673-678.
[9] Moretti J.D., Sabatini J.J., Shaw A.P., Chen G., Gilbert R.A., Jr., Promising Properties and System Demonstration of an Environmentally Benign Yellow Smoke Formulation for Hand-held Signals, *ACS Sustainable Chem. Eng*., **2014**, *2*, 1325-1330.
[10] Shimada S., Thermosonimetry and Microscopic Observation of the Thermal Decomposition of Potassium Chlorate, *Thermochim. Acta*, **1995**, *255*, 341-345.
[11] Pouretedal H.R., Ebadpour R., Application of Non-isothermal Thermogravimetric Method to Interpret the Decomposition Kinetics of $NaNO_3$, KNO_3, and $KClO_4$, *Int. J. Thermophys*., **2014**, *35*, 942-951.
[12] Rudloff W.K., Freeman E.S., The Catalytic Effect of Metal Oxides on the Thermal Decomposition of Potassium Chlorate and Potassium Perchlorate as Detected by Thermal Analysis Methods, *J. Phys. Chem.*, **1970**, *74*, 3317-3324.
[13] Yedukondalu N., Ghule V.D., Vaitheeswaran G., Pressure Induced Structural Phase Transition in Solid Oxidizer $KClO_3$: a First Principles Study, *J. Chem. Phys.*, **2013**, *138*, 174701-174708.
[14] Zhang F., Wang P., A Theoretical Study of the Thermal Decomposition Mechanism of Potassium Chlorate, *J. Beijing Univ. Chem. Technol.*, **2008**, *35*, 30-34.
[15] Nair S.M.K., Sahish T.S., Effect of Gamma-irradiation on the Thermal Decomposition of Potassium Chlorate, *J. Radioanal. Nucl. Chem.*, **1993**, *175*, 173-184.
[16] Vyazovkin S., Burnham A.K., Criado J.M., Pérez-Maqueda L.A., Popescu C., Sbirrazzuoli N., ICTAC Kinetics Committee Recommendations for Performing Kinetic Computations on Thermal Analysis Data, *Thermochim. Acta*, **2011**, *520*, 1-19.
[17] Markowitz M.M., Boryta D.A., Stewart H., The Differential Thermal Analysis of Perchlorates. VI. Transient Perchlorate Formation during the Pyrolysis of the Alkali Metal Chlorates, *J. Phys. Chem.*, **1964**, *68*, 2282-2289.

[18] Fernandez d'Arlas B., Rueda L., Stefani P.M., de la Caba K., Mondragona I., Eceiza A., Kinetic and Thermodynamic Studies of the Formation of a Polyurethane Based on 1,6-Hexamethylene Diisocyanate and Poly(Carbonate-co-Ester) Diol, *Thermochim. Acta*, **2007**, *459*, 94-103.
[19] Matečić Mušanić S., Fiamengo Houra I., Sućeska M., Applicability of Non-isothermal DSC and Ozawa Method for Studying Kinetics of Double Base Propellant Decomposition, *Cent. Eur. J. Energ. Mater.*, **2010**, *7*, 233-251.
[20] Pouretedal H.R., Damiri S., Ghaemi E.F., Non-isothermal Studies on the Thermal Decomposition of C4 Explosive Using the TG/DTA Technique, *Cent. Eur. J. Energ. Mater*., **2014**, *11*, 405-416.
[21] Georgieva V., Zvezdova D., Vlaev L., Non-isothermal Kinetics of Thermal Degradation of Chitosan, *Chem. Cent. J.*, **2012**, *6*, 1-10.
[22] Chen H., Liu N., Fan W., Two-step Consecutive Reaction Model and Kinetic Parameters Relevant to the Decomposition of Chinese Forest Fuels, *J. Appl. Polym. Sci.*, **2006**, *102*, 571-576.
[23] Kissinger H.E., Reaction Kinetics in Differential Thermal Analysis, *Anal. Chem.*, **1957**, *29*, 1702-1706.
[24] Akahira T., Sunose T., Method of Determining Activation Deterioration Constant of Electrical Insulating Materials, *Res. Report Chiba Inst. Technol. (Sci. Technol.)*, **1971**, *16*, 22-31.
[25] Lee J.-S., Hsu C.-K., Jaw K.-S., The Thermal Properties of $KClO_4$ with Different Particle Size, *Thermochim. Acta*, **2001**, *367-368*, 381-385.
[26] Vlaev L., Nedelchev N., Gyurova K., Zagorcheva M., A Comparative Study of Non-isothermal Kinetics of Decomposition of Calcium Oxalate Monohydrate, *J. Anal. Appl. Pyrolysis*, **2008**, *81*, 253-262.
[27] Li Y., Xu L., Yao X., Luo T., Liu G., Thermal Degradation Kinetics of Poly{N-[(4-bromo-3,5-difluoro)-phenyl]maleimide-co-styrene} in Nitrogen, *J. Phys.: Conf. Ser.*, **2012**, *339*, 1-8.
[28] Feng-Qi Z., Rong-Zu H., Pei C., Yang L., Sheng-Lib G., Ji-Rong S., Qi-Zhen S., Kinetics and Mechanism of the Exothermic First-stage Decomposition Reaction of Dinitroglycoluril, *Chin. J. Chem.*, **2004**, *22*, 649-652.